Mercury cycling in agricultural and managed wetlands, Yolo Bypass, California: Spatial and seasonal variations in water quality

6 authors, including:

Some of the authors of this publication are also working on these related projects:

methylmercury production View project

Reservoir Characterization View project

Mercury cycling in agricultural and managed wetlands, Yolo Bypass, California: Spatial and seasonal variations in water quality

Charles N. Alpers [a,*], Jacob A. Fleck [a,1], Mark Marvin-DiPasquale [b,2], Craig A. Stricker [c,3], Mark Stephenson [d,4], Howard E. Taylor [e,5]

[a] U.S. Geological Survey, Placer Hall, 6000 J St., Sacramento, CA 95819, United States
[b] U.S. Geological Survey, 345 Middlefield Road, Mailstop 480, Menlo Park, CA 94025, United States
[c] U.S. Geological Survey, Fort Collins Science Center, Building 21, Mailstop 963, Denver, CO 80225, United States
[d] Moss Landing Marine Laboratory, Moss Landing, CA 95039, United States
[e] U.S. Geological Survey, 3215 Marine St., Suite E-127, Boulder, CO 80303, United States

HIGHLIGHTS

- Surface water Hg chemistry was studied in agricultural and non-agricultural wetlands.
- MeHg concentrations were highest during wild-rice harvest and winter flooding.
- MeHg concentrations correlated with Mn, Fe, DOC, and $\delta^{34}S$ of dissolved sulfate.
- Sulfate-bearing fertilizer amendments had no effect on Hg(II)-methylation.

ARTICLE INFO

ABSTRACT

The seasonal and spatial variability of water quality, including mercury species, was evaluated in agricultural and managed, non-agricultural wetlands in the Yolo Bypass Wildlife Area, an area managed for multiple beneficial uses including bird habitat and rice farming. The study was conducted during an 11-month period (June 2007 to April 2008) that included a summer growing season and flooded conditions during winter. Methylmercury (MeHg) concentrations in surface water varied over a wide range (0.1 to 37 ng L^{-1} unfiltered; 0.04 to 7.3 ng L^{-1} filtered). Maximum MeHg values are among the highest ever recorded in wetlands. Highest MeHg concentrations in unfiltered surface water were observed in drainage from wild rice fields during harvest (September 2007), and in white rice fields with decomposing rice straw during regional flooding (February 2008). The ratio of MeHg to total mercury (MeHg/THg) increased about 20-fold in both unfiltered and filtered water during the growing season (June to August 2007) in the white and wild rice fields, and about 5-fold in fallow fields (July to August 2007), while there was little to no change in MeHg/THg in the permanent wetland. Sulfate-bearing fertilizer had no effect on Hg(II) methylation, as sulfate-reducing bacteria were not sulfate-limited in these agricultural wetlands. Concentrations of MeHg in filtered and unfiltered water correlated with filtered Fe, filtered Mn, DOC, and two indicators of sulfate reduction: the SO_4^{2-}/Cl^- ratio, and $\delta^{34}S$ in aqueous sulfate. These relationships suggest that microbial reduction of SO_4^{2-}, Fe(III), and possibly Mn(IV) may contribute to net Hg(II)-methylation in this setting.

Published by Elsevier B.V.

1. Introduction

Freshwater wetlands are important sites for inorganic mercury (Hg(II)) methylation and monomethylmercury (MeHg) bioaccumulation (Fitzgerald and Lamborg, 2007). For example, in the experimental lake area of Ontario, Canada, it was shown that watersheds with wetlands contributed far more MeHg than watersheds with lakes (stratified and non-stratified) and riparian habitats (St. Louis et al., 1996). Similar results have been found in other areas where seasonally flooded

* Corresponding author. Tel.: +1 916 278 3134; fax: +1 916 278 3013.
E-mail addresses: cnalpers@usgs.gov (C.N. Alpers), jafleck@usgs.gov (J.A. Fleck),
mmarvin@usgs.gov (M. Marvin-DiPasquale), cstricker@usgs.gov (C.A. Stricker),
mstephenson@mlml.calstate.edu (M. Stephenson), hetaylor@usgs.gov (H.E. Taylor).
[1] Tel.: +1 916 278 3063; fax: +1 916 278 3079.
[2] Tel.: +1 650 329 4442; fax: +1 650 329 4463.
[3] Tel.: +1 303 236 7908; fax: +1 303 236 4930.
[4] Tel.: +1 831 771 4170; fax: +1 831 633 0128.
[5] Tel.: +1 303 541 3007; fax: +1 303 541 3084.

wetland habitats can have particularly high MeHg (e.g. Bradley et al., 2011; Rudd, 1995).

Rice paddies are among the most abundant wetland ecosystems in temperate and tropical latitudes worldwide. In California, rice is planted on about 200,000 ha (California Rice Commission, 2012), which is about 2.5 times greater than remaining seasonal and semi-permanent natural wetlands (Central Valley Joint Venture, 2006). Because the hydroperiod of seasonal and agricultural wetlands is highly dynamic, these habitats can be potentially important sites of Hg(II)-methylation (e.g. Horvat et al., 2003; Rothenberg and Feng, 2012; Snodgrass et al., 2011) and sources of MeHg, which is subject to bioaccumulation and/or export to downstream habitats. It has been demonstrated that addition of sulfate can stimulate MeHg production in wetlands (e.g. Jeremiason et al., 2006; Orem et al., 2011), yet to date there have been no studies of the effects of sulfate-bearing fertilizer on Hg cycling in rice paddies.

Managed wetlands in the Yolo Bypass Wildlife Area (YBWA) were selected for this study because they fall along a spectrum of hydrologic management within close proximity, including quasi-natural seasonal and permanent wetlands (non-agricultural) as well as white rice, wild rice, and fallow agricultural fields (Windham-Myers et al., in this issue-a). Additionally, the YBWA wetlands represent an important habitat within the Pacific Flyway, a migratory waterfowl corridor of many thousands of ha of wetlands throughout California (Elphick, 2000). Furthermore, the Yolo Bypass is known to be contaminated with Hg (Heim et al., 2007) from historical mining of Hg in the California Coast Ranges (Domagalski et al., 2004; Rytuba, 2003) and gold (Au) in the Sierra Nevada mountains, where Hg–Au amalgamation was used extensively at both placer and hardrock mines (Alpers et al., 2005).

The Yolo Bypass is an important source of Hg and MeHg to the Sacramento–San Joaquin Delta (Springborn et al., 2011), an area with fish-consumption advisories for Hg (Davis et al., 2003), and demonstrated adverse effects on bird reproduction (e.g. Ackerman et al., 2008). Previous work in the YBWA wetlands showed elevated concentrations of MeHg in water and sediment (Marvin-DiPasquale et al., 2009). Resource managers have concerns that any changes to restore the Delta, including a proposal to create thousands more hectares of wetlands, will exacerbate the Hg problem (e.g. Wood et al., 2010).

The primary objectives of this study were to quantify and compare Hg and MeHg concentrations in YBWA surface waters from different wetland types including agricultural (rice-growing) and non-agricultural wetlands, and to determine the dominant processes that lead to Hg(II)-methylation under different land-management practices. To address these objectives, we evaluated the hypothesis that Hg(II)-methylation is influenced by seasonal and spatial variations in the activity of sulfate-reducing and iron- (Fe-) reducing bacteria (SRB and FeRB), and we postulated that such variations are manifested in seasonal and spatial variations in water quality. A secondary objective of this study was to determine whether or not the amendment of sulfate-bearing fertilizer stimulates microbial sulfate reduction and Hg(II)-methylation in fertilizer-amended rice fields. To address this, we evaluated the hypothesis that processes affecting surface-water sulfate concentrations (fertilization, sulfate reduction, and evaporation) can be quantified using concentration ratios (e.g. sulfate concentration normalized by chloride, SO_4^{2-}/Cl^-) and stable isotopes (e.g. $\delta^{34}S$ of sulfate and $\delta^{18}O$ of water). We also tested the null hypothesis that no significant difference in surface-water MeHg between fertilized and unfertilized fields indicates that sulfate addition did not stimulate additional SRB-related Hg(II)-methylation.

This study is part of an integrated, multi-disciplinary approach involving concomitant sampling of surface water, sediment, pore water, plants, and biota, described in detail by Windham-Myers et al., in this issue-a. Water quality is an essential aspect of the multi-disciplinary study of Hg cycling in wetlands because water is the main transport agent for Hg and MeHg between the sediment, plant, and biota compartments. Results regarding total mercury (THg) and MeHg concentrations in wetland surface waters and related biogeochemical processes

are reported here; results on exported loads of THg and MeHg from the wetlands and hydrological processes affecting the mass balance of THg and MeHg are reported separately (Bachand et al., in this issue-a,-b). Both in situ (within the YBWA) concentrations and exports are important controls on the exposure of local biota to THg and MeHg (Ackerman and Eagles-Smith, 2010; Ackerman et al., 2010), whereas exports may additionally impact sensitive downstream environments (Davis et al., 2003). Photodegradation of MeHg in the YBWA is described by Fleck et al. (in this issue). Biogeochemical processes in sediment, including plant–soil interactions, are described by Marvin-DiPasquale et al. (in this issue) and Windham-Myers et al. (in this issue-b,-c).

2. Materials and methods

2.1. Collection and preservation of water samples

Surface-water samples were collected from three agricultural wetland types (white rice, wild rice, and fallow fields), a non-agricultural seasonal wetland, and a permanent wetland within the YBWA over the course of an annual cropping sequence during 2007 to 2008. For each of the three agricultural wetland types, two separate fields were sampled (Table S1; table and figure numbers beginning with "S" are provided as Supplemental Material). Water samples were taken at wetland inlets, centers, and outlets at a frequency of twice per month during the growing season (June–August 2007), and more frequently (6 per month) during the harvest of wild rice (September 2007). Wild rice was harvested during wet conditions to maximize production by preventing the drying out of plants and associated "shattering" of rice kernels (California Wild Rice Advisory Board, 2012). In contrast, the white rice fields were drained (during September 2007) prior to harvest. During autumn, approximately one sample was taken per month as field conditions allowed. During winter flooding (December 2007–April 2008), one to six samples were taken per month in each field (Table S1). Regional flooding of the Yolo Bypass affected site conditions during late January to mid-February 2008 (Windham-Myers et al., in this issue-a).

The field sampling plan consisted of three levels of intensity with regard to water-quality sampling and analyses: Schedules A, B, and C (Table S2). Schedule A was executed at field centers in coordination with sediment and plant sampling, consistent with the study goal of providing a holistic view of Hg cycling in YWBA wetland habitats. Schedule A samples were collected at five time points indicative of the dominant management activities in the wetlands under study, including initial flooding and starter fertilizer application (June 2007), mid-irrigation-season and top dressing fertilizer application, (July 2007), pre-harvest (August 2007), winter flood-up (Dec. 2007, prior to regional flood) and winter drainage (Feb. 2008, after regional flood). Schedule B sampling collected the same water-quality constituents as Schedule A, but without the concomitant sampling of sediment and plants. Schedule B samples were taken at field inlets and outlets at the same time as the five Schedule A sampling events plus on 10 other occasions. Water sampling locations at wetland inlets and outlets coincided as closely as possible with hydrologic measurements to facilitate load calculations (Bachand et al., in this issue-a,-b). Schedule C samples were taken at inlets and outlets, temporally between the Schedule A and B sample collections (e.g. June–Aug. 2007, Nov. 2007, Jan. 2008) and during drainage events (Sept. 2007, Mar. 2008), and were analyzed for a subset of the analytes in Schedules A and B (Table S2), including unfiltered MeHg (MeHg-U), dissolved organic carbon (DOC), sulfate (SO_4^{2-}), and chloride (Cl^-), to provide greater certainty in load calculations (see Bachand et al., in this issue-b). In situations where wetlands had multiple inlets or outlets, water samples were composited in proportion to flow at each location.

Water-quality field measurements taken during sample collection included pH, dissolved oxygen, water temperature, and specific conductance. Measurements were made in situ near sample collection points

using a multi-parameter sonde (YSI model 6920v2). Water samples were collected using a 3-L Teflon® bottle tethered to a clean PVC sampling rod with plastic ties. For Schedules A and B, the water was transferred to an acid-cleaned, 13-L Teflon®-lined (fluorinated) plastic container according to 'clean-hands' methods (U.S. EPA Method 1669). Replicate water samples were taken by filling two 13-L containers simultaneously. To fill the 13-L containers, half of each 3-L Teflon® collection bottle was poured into each of the replicated containers. The water samples were stored on wet ice, transported to the U.S. Geological Survey (USGS) California Water Science Center (CAWSC) laboratory in Sacramento, CA, and refrigerated to less than 5 °C.

Sample processing was completed within 24 h of collection. Schedule A and B samples were split in the laboratory using a 20-L acid-cleaned, Teflon®-lined, stainless-steel churn splitter. Aliquots for all unfiltered analyses were collected from the churn prior to the collection of any filtered aliquots to minimize bias with regard to suspended sediment concentration. Schedule C sample bottles for MeHg-U and total suspended solids (TSS) were filled and preserved in the field. A single 2-L or 3-L sample was collected for the remaining analytes processed at the USGS Sacramento laboratory using the same methods as performed for Schedules A and B.

For THg, MeHg, and all other analytes other than DOC, a capsule filter (Gelman) with a nominal pore size of 0.45 μm was used. For DOC, a quartz-fiber filter with nominal pore size of 0.3 μm was used. Subsamples for analysis of THg and MeHg, both unfiltered and filtered, were preserved using ultrapure HCl to an approximate final concentration of 0.5%. Subsamples for analysis of iron (Fe) and manganese (Mn) were preserved using triple-distilled HNO_3 to an approximate final concentration of 1%. Filtered subsamples for analysis of S isotopes in aqueous sulfate were shipped to the USGS stable-isotope laboratory in Denver, CO, where sulfate was precipitated as $BaSO_4$ following acidification, heating, and addition of excess $BaCl_2$. Subsamples of unfiltered water for stable H and O isotope analyses were collected into 60 mL conical cap glass bottles with minimal head space.

2.2. Laboratory analyses

Analytical methods, parameter abbreviations, and reporting units are listed in Table S3. Reference citations for analytical methods not discussed here are in the Supplemental Material.

The following forms of Hg in water were determined for this study: (1) THg in unfiltered water (THg-U), (2) THg in filtered water (THg-F), (3) MeHg-U, and (4) MeHg in filtered water (MeHg-F). Square brackets are used throughout to signify concentration, e.g. [THg-U]. The volumetric concentration of particulate total mercury [THg-P_V] was calculated as the difference between [THg-U] and [THg-F]. Similarly, the volumetric concentration of particulate methylmercury [MeHg-P_V] was calculated as [MeHg-U] − [MeHg-F] (Table S3). Total Hg and MeHg were determined using EPA methods 1631 (revision E) and 1630, respectively, at the Moss Landing Marine Laboratory (MLML) in Moss Landing, CA.

Method detection limits (MDL) were 0.2 ng L^{-1} for THg and 0.02 ng L^{-1} for MeHg. Details on quality assurance and quality control for Hg species and other analytes are available in the Supplemental Material (Tables S4.1–S4.12) and are summarized in Table 1, which includes information on detection limits, field blanks, replicates, standard reference materials, matrix spikes, and matrix spike duplicates.

The concentration of suspended material in the water column was quantified using two methods: TSS was determined at MLML and suspended particulate matter (SPM) was determined at the USGS CAWSC. Total suspended sediment was determined using Standard Method 2540 D. A subsample of 100 mL was drawn using a pipette from a 1-L sample during homogenization using a magnetic stirrer; the water was then passed through a standard glass-fiber filter (0.7 μm nominal pore size, pre-combusted at 500 °C), which was subsequently dried at 103–105 °C. The dried filter was weighed and the increase in mass was divided by the subsample volume to determine [TSS]. The TSS MDL was 3.0 mg L^{-1}. The median relative percent difference (RPD) for TSS field replicates was 11% with a standard deviation of 50%, with higher RPD values noted at lower concentrations.

Suspended particulate matter was determined using a filtration method at the USGS CAWSC research laboratory in Sacramento. A pre-weighed filter (glass fiber, 0.7 μm nominal pore size, pre-combusted at 500 °C) was loaded into a clean Teflon® filter holder. A well-mixed aliquot (20 to 200 mL) was poured from the churn into a graduated cylinder to obtain an accurate volume for filtration, with larger volumes required for less turbid samples. The aliquot was poured quickly from the graduated cylinder into the Teflon® filter tower to minimize settling within the cylinder. Most samples were allowed to filter by gravity; however, in some instances a light vacuum (<5 psi) was required. The loaded filter was placed into a petri dish and frozen for storage. Filters were dried at 105 °C, placed in a desiccator for cooling, and reweighed. After subtracting the original mass of the filter, the final mass was divided by the volume filtered to obtain volumetric [SPM] (in mg L^{-1}). The median RPD for SPM field replicates was 5% with a standard deviation of 26%. The high standard deviation was due to three replicates (out of 30) with very high concentration (>150 mg L^{-1}), for which small sample volumes reduced precision. Higher uncertainty at higher concentration is consistent with known limitations of this method. Most samples in this study met criteria for acceptable use of this method.

The gravimetric concentration of particulate MeHg [MeHg-P_G] was computed as [MeHg-P_V] / [SPM], in units of μg g^{-1}. Similarly, [THg-P_G] was computed as [THg-P_V] / [SPM].

The partitioning among particulate and dissolved forms of THg and MeHg is described by partitioning coefficients (K_d). For MeHg, the K_d was calculated as:

$$K_{d,MeHg} = ([MeHg\text{-}P_V]/[SPM])/[MeHg\text{-}F] = [MeHg\text{-}P_G]/[MeHg\text{-}F] \quad (1)$$

Table 1
Summary of quality assurance and quality control data. RPD, relative percent difference; n, number of observations. For definitions of parameters, see text or Table S3.

	THg-U	THg-F	MeHg-U	MeHg-F	SO_4^{2-}	Cl^-	ALK	Br^-	Fe	Mn	DOC
Method detection limit and units	0.2 ng L^{-1}	0.2 ng L^{-1}	0.02 ng L^{-1}	0.02 ng L^{-1}	0.18 mg L^{-1}	0.12 mg L^{-1}	1 mg L^{-1}	0.02 mg L^{-1}	2 μg L^{-1}	0.05 μg L^{-1}	0.3 mg L^{-1}
Field blanks (median concentration, n)	<MDL (6)	<MDL (6)	<MDL (14)	<MDL (6)	<MDL (9)	<MDL (9)	na	<MDL (6)	3.9 (23)	0.07 (3)	<MDL (20)
Replicates (median RPD, n)	5.9% (12)	8.9% (12)	13% (26)	7.6% (12)	0.2% (27)	0.3% (27)	0.3% (9)	0.8% (12)	9.8% (11)	2.0% (9)	1.3% (28)
Standard reference materials (median % recovery, n)	95.6% (10)	na	96.5% (30)	na	99.3% (6)	101% (6)	na	100.4% (4)	91.9% (16)	100.5 (24)	99.0% (29)
Matrix spikes (median % recovery, n)	94.4% (10)	na	100% (30)	na	97.5% (10)	99.3% (10)	na	93.1% (3)	100.9% (3)	107.1 (4)	101% (7)
Matrix spike duplicates (median RPD, n)	2.0% (10)	na	4.8% (30)	na	0.2% (10)	0.05% (10)	na	1.2% (3)	na	na	6.0% (3)

where [MeHg-P$_V$] and [MeHg-F] are in units of ng L^{-1} and SPM is in units of kg L^{-1}, so that $K_{d,MeHg}$ is in units of L kg^{-1}. The K_d for THg ($K_{d,THg}$) was calculated similarly:

$$K_{d,THg} = ([THg-P_V]/[SPM])/[THg-F] = [THg-P_G]/[THg-F]. \qquad (2)$$

Concentrations of SO$_4^{2-}$, Cl$^-$, and Br$^-$ were determined by ion chromatography at the USGS laboratory in Denver, CO (Tables S3, S5.7). Concentrations of Fe and Mn were determined by ICP-MS at the USGS laboratory in Boulder, CO (Tables S3, S5.8). Data on nutrients (various forms of nitrogen and phosphorus) are available at http://nwis.waterdata.usgs.gov/nwis. The concentration of DOC and optical properties of dissolved organic matter (DOM) were determined using methods described by Fleck et al. (in this issue). Specific ultraviolet absorbance at 254 nm (SUVA$_{254}$ in units of L mg^{-1} m^{-1}), an indicator of DOM aromaticity, was calculated by normalizing absorbance at 254 nm to [DOC].

Stable isotope ratios of hydrogen (^{2}H/^{1}H) and oxygen (^{18}O/^{16}O) in water were determined using standard methods (Coleman et al., 1982; Epstein and Mayeda, 1953) at the USGS stable isotope laboratory in Denver, CO. Oxygen isotope ratios in water, expressed as δ^{18}O in units of parts per thousand (‰) relative to Vienna Standard Mean Ocean Water (VSMOW), were determined by dual inlet mass spectrometry after equilibration with carbon dioxide. Hydrogen isotope ratios, expressed as δD in units of ‰ relative to VSMOW, were determined by dual inlet mass spectrometry after quantitative conversion to H$_2$ by the zinc shot technique. Hydrogen and oxygen isotope data were normalized to VSMOW (δD = 0‰; δ^{18}O = 0‰) and SLAP (δD = −428‰; δ^{18}O = −55.5‰). Calibrated working standards were analyzed in duplicate with each batch for quality assurance. Analytical uncertainty was ± 0.05‰ for δ^{18}O and ± 1.0‰ for δD.

Stable isotope ratios of sulfur (^{34}S/^{32}S) in aqueous sulfate were analyzed at the USGS stable isotope laboratory in Denver, CO, by continuous flow isotope ratio mass spectrometry where BaSO$_4$ precipitates were quantitatively converted to SO$_2$ using an elemental analyzer (Carmody et al., 2008; Kester et al., 2001). Sulfur isotopes in aqueous sulfate are expressed as δ^{34}S$_{SO4}$ and are reported relative to the Vienna Cañon Diablo Troilite (VCDT) using internationally accepted standards (IAEA-SO-6 = −34.1‰, NBS127 = 21.1‰). Analytical uncertainty was ± 0.2‰ for δ^{34}S$_{SO4}$.

2.3. Meteorological data

Meteorological data were obtained from the California Irrigation Management System (http://wwwcimis.water.ca.gov) site #6, Davis (N38°32′09″, W121°46′32″) which is located approximately 11 km west of the YBWA.

2.4. Statistical analyses

Normality of data was assessed using the Shapiro–Wilk test (SigmaPlot, version 11, Systat Software, Inc., San Jose, Calif.). Nearly all data were non-normal even with log transformation, so nonparametric statistics were used; median values and the interquartile range (25% to 75% of distribution) are typically reported. Correlation coefficients (r_S) for relationships among variables were determined using Spearman rank order (SigmaPlot, v. 11). Correlations were considered significant when type-II error probability (p) was <0.1. In cases where p values were smaller (e.g. <0.05, <0.01, <0.001, or <0.0001) the value is given, indicating a higher probability that the distribution is not caused by chance (the null hypothesis). Values of r_S are reported only for significant correlations. The non-parametric Mann–Whitney test was applied (using SigmaPlot v. 11) to various subgroups of the water-quality data to assess whether or not statistically significant differences were found. Linear least-squares regressions were made

using SigmaPlot (v. 11). Summary statistics, including median and interquartile range (Table S6), were generated using S+ (Release 8.1; TIBCO Software Inc., Palo Alto, Calif.).

3. Results and discussion

Data for various water-quality constituents and fertilizers are provided in the Supplemental Material (Tables S5.1–S5.11).

3.1. Mercury, methylmercury, organic matter, and suspended particulate matter

3.1.1. Relationships among mercury species

Considering all of the water samples taken over the course of the study, concentrations of THg and MeHg ranged over approximately two orders of magnitude for both filtered and unfiltered samples (Fig. 1). The proportion of filter-passing MeHg, expressed as the ratio of filtered to unfiltered MeHg ([MeHg-F]/[MeHg-U]), varied from about 10% to 100% (Fig. 1A). The median value of [MeHg-F]/[MeHg-U] was 41% and the interquartile range (25th to 75th percentile) was 28% to 63%. At higher concentrations ([MeHg-U] > 4 ng L^{-1} and [MeHg-F] > 2 ng L^{-1}), the values of [MeHg-F]/[MeHg-U] were uniformly >40%. The r_S between [MeHg-U] and [MeHg-F] was 0.77, the highest value among filtered and unfiltered THg and MeHg species (Fig. 1). It is possible that some of the MeHg-F represents colloidal particles that passed though the capsule filter. The relatively strong correlation between [MeHg-U] and [MeHg-F] is similar to the relationship described in a tidal wetland in the San Francisco Bay-Delta estuary (Bergamaschi et al., 2011).

The proportion of filter-passing THg ([THg-F]/[THg-U]) ranged from about 5% to about 95% (Fig. 1B), with a median of 33% and interquartile range of 16% to 42%, indicating that THg was more associated with SPM than was MeHg. The proportion of [THg-F]/[THg-U] was relatively low in the permanent wetland (5 to 50%), relatively high in the seasonal wetland (30 to 95%), and highly variable (5 to 95%) in the agricultural fields. Mercury in the dissolved and colloidal (filter-passing) forms has a greater potential for further cycling and transport than Hg bound to filterable suspended sediment (e.g. Hammerschmidt and Fitzgerald, 2004; Zhang et al., 2012).

During the study period, [THg-U] exceeded the EPA water-quality criterion of 50 ng L^{-1} (California Toxics Rule; U.S. EPA, 2000) in 11 of 105 samples (10.5%), especially following the initial flooding of the agricultural wetlands and following the regional flooding of the Yolo Bypass (Fig. 1B–C). Although the water-quality criterion in the California Toxics Rule is not typically enforced in agricultural systems, it indicates potentially important sources of THg to downstream environments. There are no regulatory criteria for MeHg, however, Rudd (1995) indicated that [MeHg-U] > 0.1 ng L^{-1} is considered elevated and likely to lead to significant MeHg bioaccumulation. Within the Sacramento–San Joaquin Delta, there is a regulatory TMDL goal for [MeHg-U] of 0.06 ng L^{-1} (Wood et al., 2010). All of the MeHg-U concentrations determined in this study (234 of 234, 100%) equaled or exceeded 0.1 ng L^{-1} (Fig. 1, Table S5.2), confirming conclusively that the YBWA is an area of elevated MeHg exposure. The high values of [MeHg-U] observed in this study (up to 37 ng L^{-1} at the outlet of wild rice fields during harvest; Figs. S1, S2A–B) are similar in magnitude to the "unprecedented" values (up to 20 ng L^{-1}) observed in a wetland designed to treat runoff in the northern Everglades (Rumbold and Fink, 2006).

The proportion of THg that was MeHg in unfiltered water ([MeHg-U]/[THg-U]) ranged from about 1% to 80% (Fig. 1C), with a median of 6.4%; the interquartile range was 6 to 17%. In filtered water, [MeHg-F]/[THg-F] also ranged from about 1% to 80% but the median and interquartile range were higher (17%, and 7 to 27%, respectively; Fig. 1D). At lower concentrations (i.e. [THg-F] < 3 ng L^{-1} and [MeHg-F] < 0.5 ng L^{-1}) values of [MeHg-F]/[THg-F] were in a narrower range, from about 5 to
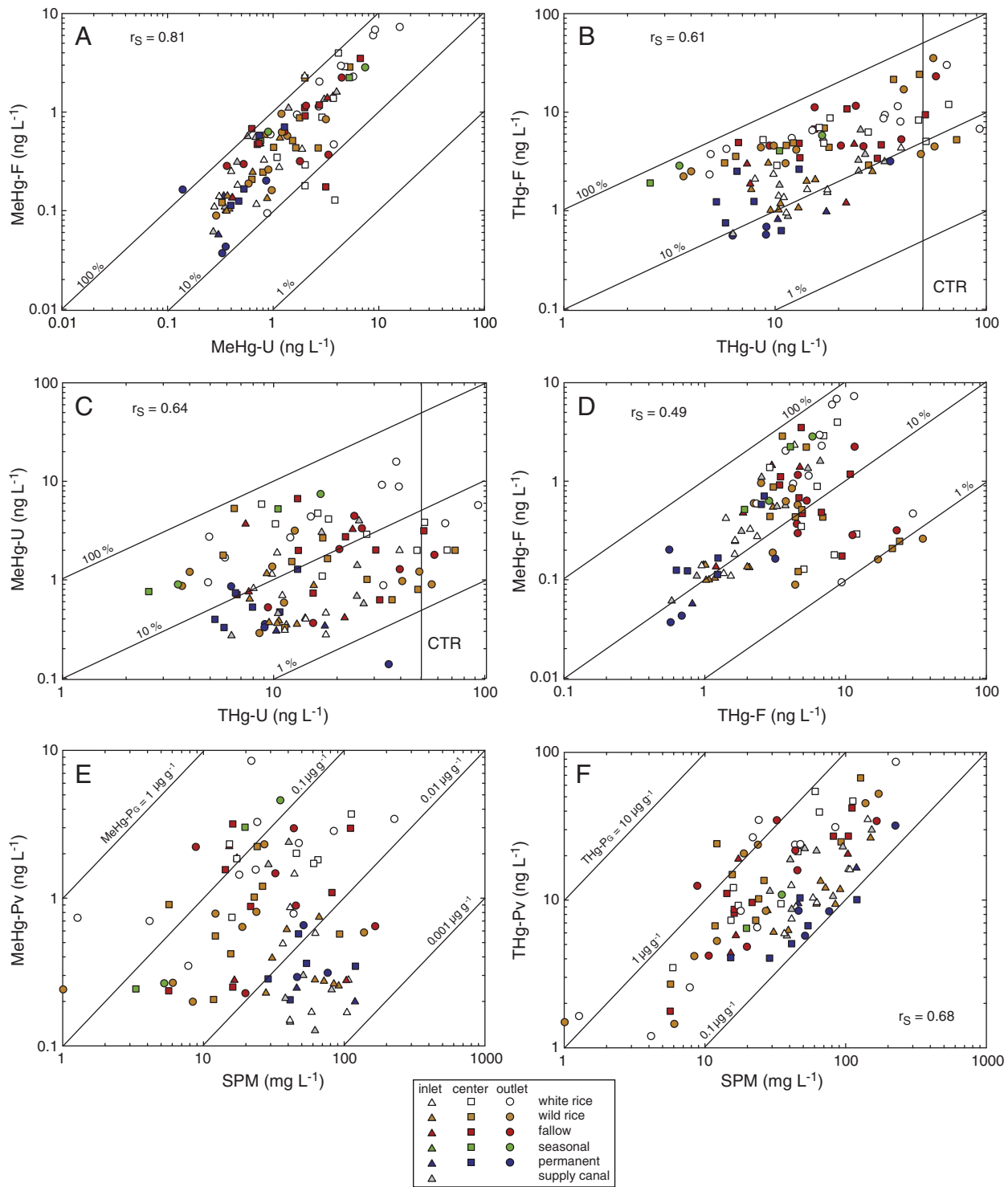
Fig. 1. Scatter plots showing data for total mercury (THg), methylmercury (MeHg), and suspended particulate matter (SPM) in surface-water samples in agricultural and non-agricultural wetlands in the Yolo Bypass Wildlife Area, California. A) unfiltered MeHg (MeHg-U) vs. filtered MeHg (MeHg-F), B) unfiltered THg (THg-U) vs. filtered THg (THg-F), C) THg-U vs. MeHg-U, D) THg-F vs. MeHg-F, E) SPM vs. particulate MeHg (MeHg-P), and F) SPM vs. particulate THg (THg-P). In A) and B), diagonal lines represent ratio of filtered to unfiltered concentration, in percent. In C) and D), diagonal lines represent ratio of MeHg to THg, in percent. In E) and F), diagonal lines represent concentration of MeHg or THg on suspended particulates, in parts per million (ng mg^{-1} or μg g^{-1}). CTR indicates California Toxics Rule regulatory criterion for THg-U (50 ng L^{-1}; U.S. EPA, 2000). Values of r_S are Spearman rank order coefficients, shown where correlations are statistically significant (p < 0.05).

50%. The observed proportions of MeHg/THg in filtered and unfiltered water are relatively high compared with other environments such as rivers in unmined areas (e.g. Balogh et al., 2008; Brigham et al., 2009), rivers in mined areas (e.g. Ganguli et al., 2000; Gray et al., 2002, 2004), reservoirs (e.g. Alpers et al., 2008), and boreal wetlands (e.g. St. Louis et al., 1994), but are typical for some organic-rich wetland environments such as rivers in the South Carolina coastal plain (e.g. Guentzel, 2009).

3.1.2. Relationships among mercury species and organic matter

Relationships between DOM and various forms of aqueous Hg were highly variable in both space and time during this study. Filtered total mercury [THg-F] was closely related to [DOC], but varied over the three distinct periods of field conditions, as described in detail in the Supplemental Material (Section S1). In short, different ranges of [THg-F]/[DOC] were observed during the discrete hydro-periods of water management (Fig. S2). Higher values of [THg-F]/[DOC] were observed in the agricultural wetlands during the early part of the growing season (June–July 2007) and after a regional flood (February–April 2008), whereas lower values of [THg-F]/[DOC] occurred during the latter part of the growing season and the initial winter flood (July 2007–January 2008).

Correlations between [DOC] and [MeHg-F] were weaker than those between [DOC] and [THg-F], but were statistically significant during two of the three periods described above. Highest values of [MeHg-F]/[DOC] were observed after the regional flood. These observations underscore the complexity of DOM-THg-MeHg interactions in managed wetland systems.

3.1.3. Relationships between mercury species and suspended particulate matter

Values of [MeHg-P_V] did not correlate significantly with SPM; [MeHg-P_G] spanned about two orders of magnitude, from about 0.002 to 0.2 $\mu g\ g^{-1}$ (Fig. 1E). In contrast, [THg-P_V] correlated with SPM ($r_S = 0.68$) and [THg-P_G] spanned a little more than one order of magnitude, from about 0.1 to 2 $\mu g\ g^{-1}$ (Fig. 1F). Samples from the permanent wetland were relatively low in all four particulate concentrations: MeHg-P_V, THg-P_V, MeHg-P_G, and THg-P_G. The seasonal wetland was relatively low in THg-P_G (about 0.3 $\mu g\ g^{-1}$) but among the highest in MeHg-P_G (around 0.2 $\mu g\ g^{-1}$). This is consistent with the seasonal wetland having among the highest values of [MeHg-U]/[THg-U] (Fig. 1C).

Values of [MeHg-P_G] ranged from approximately 0.002 to 0.2 $\mu g\ g^{-1}$ (Fig. 1E, Table S5.2); the median value of [MeHg-P_G] was 0.024 $\mu g\ g^{-1}$, with an interquartile range of 0.005 to 0.067 $\mu g\ g^{-1}$. These concentrations are about ten-fold higher than MeHg in concurrently collected bed sediment (0–2 cm depth), which had a median MeHg concentration of 0.002 $\mu g\ g^{-1}$ and an interquartile range of about 0.001 to 0.003 $\mu g\ g^{-1}$ (Marvin-DiPasquale, in this issue). There was a significant correlation ($r_S = 0.63$, p < 0.0001) between MeHg-P_G and the organic content of the SPM, measured as LOI (Fig. S4B). These results suggest that there may be uptake of MeHg on organic-rich suspended particles representing phytoplankton (e.g. Pickhard and Fisher, 2007), periphyton, or biofilm (e.g. Lin and Jay, 2007).

Partitioning of THg and MeHg between suspended particulates and the dissolved phase, expressed as K_d values is described in detail in Section S2. In short, values of $K_{d,THg}$ and $K_{d,MeHg}$ varied systematically with [SPM] (Table 2, Fig. S3); this may be caused by a "particle concentration effect" similar to that observed in other studies (e.g. Brigham et al., 2009; Turner and Millward, 2002), whereby colloidal particles pass through filters and contribute to the "dissolved" phase disproportionately at high [SPM]. Suspended particulates had higher organic content (measured as LOI) at lower SPM concentration (Fig. S4); in

these conditions, much of the SPM is algae, which may favor MeHg partitioning onto suspended particulates.

3.1.4. Spatial and seasonal variations

At the centers and outlets of the white and wild rice fields, both [MeHg-U] and [MeHg-F] increased over time during the growing season, from June to August (Figs. S1, S5A–B). During the post-harvest period, comparing data from December 2007 to those from February 2008, [MeHg-F] increased through time at the centers and outlets of most wetlands (Figs. S1, S5B), a temporal trend that was similar to the trend described for sediment MeHg in field centers (Marvin-DiPasquale et al., in this issue). Data from field centers and outlets were pooled for this analysis, as no significant differences were observed when comparing concentrations of MeHg and THg (Mann–Whitney rank sum test). Also, no significant differences were found in the overall data set (centers and outlets) between agricultural and non-agricultural wetlands with regard to MeHg/THg in either unfiltered or filtered water (Mann–Whitney test).

The highest values for both [MeHg-U] and [MeHg-F] were observed in white rice fields (centers and outlets) during the growing season (June–August 2007) and the post-harvest season (February 2008), following the regional flood and during the period when rice straw was decomposing. Elevated [MeHg-U] values (up to 37 ng L^{-1}) were observed in wild rice field outlets (Table S5.2; Figs. S1, S5A–B) with an average value of 12 ng L^{-1} during harvest (September 2007). The permanent wetland maintained relatively low [MeHg-U] and [MeHg-F] throughout the year, except when inundated by floodwaters that covered much of the YBWA in early February 2008. The latter results are consistent with other studies that have pointed out the importance of hydro-period (wet/dry cycles) with regard to Hg(II)-methylation (e.g. Snodgrass et al., 2011).

In contrast to [MeHg], both [THg-U] and [THg-F] decreased with time during the growing season (June–August 2007) at centers and outlets of white and wild rice fields (Fig. S5C–D). In fallow fields (which were dry during June 2007), both [THg-U] and [THg-F] decreased from July to August (Fig. S5C–D). The initial pulse of elevated THg during the growing season was about 50% in the filtered fraction [THg-F], whereas the elevated THg during the post-harvest season was associated with higher concentrations of SPM (Fig. S3C). The pulse of elevated [MeHg-U] that occurred during harvest of the wild rice fields, in September 2007 (Figs. S1, S2A, and S5A–B), was not accompanied by elevated [SPM] (Fig. S6C), so it was associated either with dissolved MeHg or filter-passing colloids.

The ratio of MeHg to THg (MeHg/THg), often used as a measure of Hg(II)-methylation efficiency (e.g. Krabbenhoft et al., 1999), increased about 20-fold for both unfiltered and filtered water during the growing season (June–August) in the white and wild rice fields, and about 5 fold in the fallow fields (July–August), while there was little to no change in this ratio in the permanent wetland (Fig. S2E–F). Values of [MeHg-F]/[THg-F] increased on all field types by about 2 fold during the post-harvest period (December to February) (Fig. S2F), but was statistically significant only on the fallow fields (Mann–Whitney test).

Table 2
Spearman rank order correlation coefficients (r_S) for mercury parameters in relation to selected water-quality constituents. ns, not significant (p > 0.1); italics, 0.05 < p < 0.1; regular font, p < 0.05; bold, r_S > 0.5 or < −0.5. For definitions and units of parameters, see Table S3. For number of observations for each correlation, see Table S10.

	MeHg-U	MeHg-F	THg-U	THg-F	(MeHg/THg)-U	(MeHg/THg)-F	log $K_{d,MeHg}$	log $K_{d,THg}$
SO_4^{2-}/Cl^-	−0.27	−0.26	0.21	ns	−0.40	−0.35	ns	*−0.18*
$\delta^{34}S$ in sulfate	0.39	0.26	ns	ns	0.38	0.30	ns	*0.19*
SPM	ns	−0.27	**0.54**	−0.24	**−0.56**	ns	**−0.51**	ns
DOC	0.50	0.24	ns	**0.60**	0.41	ns	**0.54**	−0.23
Fe	0.26	**0.50**	ns	*0.17*	0.35	0.43	*−0.21*	−0.23
Mn	**0.65**	**0.72**	ns	0.35	**0.52**	**0.57**	ns	−0.22
Days since flood	ns	ns	**−0.67**	**−0.64**	0.36	**0.59**	−0.41	**0.60**

Values of [THg-U] and [THg-F] were consistently higher in center and outflow samples from agricultural wetlands compared with those from non-agricultural wetlands (Mann–Whitney test) (Fig. S9). The means (±std. dev.) for [THg-U] were 27.8 ± 20.8 ng L^{-1} agricultural and 10.2 ± 8.1 ng L^{-1} non-agricultural; for [THg-F], 7.9 ± 6.9 ng L^{-1} agricultural and 2.05 ± 1.57 ng L^{-1} non-agricultural. Differences in aqueous THg between agricultural and non-agricultural wetlands coincide with a general east–west gradient (lower in east, higher in west) noted in sediment THg concentrations (Marvin-DiPasquale et al., in this issue; see map in Windham-Myers et al., in this issue-a). The east–west gradient in THg likely reflects the sediment source with high-THg sediment from Cache Creek deposited in the western part of the YBWA, and lower THg sediment of the Sacramento River dominating deposition in the eastern portion (Sommer et al., 2008). Values of [MeHg-U] and [MeHg-F] were also significantly higher in the agricultural fields (Fig. S9). The means (±std. dev.) for [MeHg-U] were 3.3 ± 4.4 ng L^{-1} agricultural and 1.5 ± 1.8 ng L^{-1} non-agricultural; for [MeHg-F], 1.3 ± 1.6 ng L^{-1} agricultural and 0.61 ± 0.87 ng L^{-1} non-agricultural.

3.1.5. Inlets vs. outlets

Evapoconcentration was quantified using two independent approaches: (1) [Cl$^-$], and (2) δ^{18}O and δD. Because chloride is considered to be a conservative ion in freshwater systems, it tends to be concentrated in surface water in direct proportion to the amount of evaporation (Drever, 1997). Additionally, water isotopes show a systematic trend with evaporation, yielding a characteristic slope between 3 and 5, in contrast to unevaporated waters which tend to approximate the Global Meteoric Water Line with a slope of 8 (Clark and Fritz, 1997). A plot of δ^{18}O versus δD for water samples collected in this study (Fig. 2A) shows a slope of 4.75, which demonstrates that surface waters were evaporated. The empirical fractionation factor, α, is equal to 1.009 for δ^{18}O during evaporation (Clark and Fritz, 1997). On a log-linear plot of chloride concentration versus δ^{18}O, the expected slope for water affected by evapoconcentration, based on Rayleigh fractionation (Clark and Fritz, 1997) is 20.7 (i.e., 9 ∗ 2.303). The data from this study plot in a distribution very close to the expected slope (m = 20.1) (Fig. 2B), which corresponds to an empirical α value of 1.0087 (20.1 divided by 2.303). These data (Fig. 2) provide evidence that chloride behaves as a conservative tracer in this system and therefore can be used to normalize other constituents to account for evapoconcentration effects. This approach is extended by Bachand et al. (in this issue-a,-b) who use chloride to distinguish between effects of evaporation and transpiration, to normalize load calculations, and to compute mass balances.

Unfiltered methylmercury [MeHg-U] increased significantly from inlet to outlet in all rice fields and in the seasonal wetland; however, there was no significant increase in fallow fields or in the permanent wetland (Fig. 3A). The same relationships were found for [MeHg-U]/[Cl] (Fig. 3B), which indicates that increases in MeHg caused by in-field processes other than evapoconcentration were significant.

The lack of increase in MeHg-U from inlet to outlet in the permanent wetland may relate to demethylation processes being more dominant
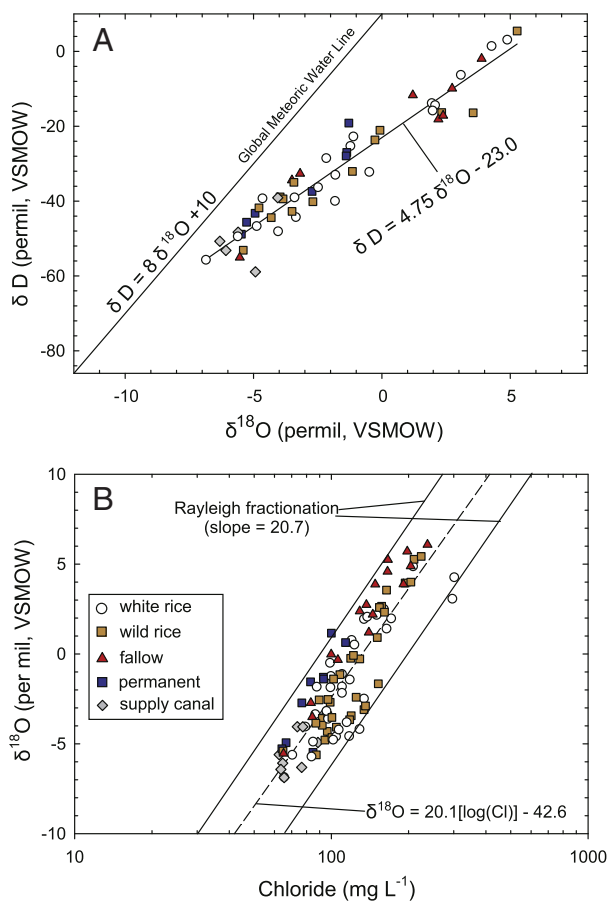

Fig. 2. Plots showing data for stable isotopes in water samples from agricultural and non-agricultural wetlands in the Yolo Bypass Wildlife Area, California for samples taken during the summer rice-growing season. A) δ^{18}O vs. δD, B) chloride vs. δ^{18}O. In A), linear least-squares regression ($r^2 = 0.93$) with slope of 4.75 indicates evaporation compared with Global Meteoric Water Line with slope of 8 (Craig, 1963). In B), linear least-squares regression ($r^2 = 0.76$) compared with theoretical lines indicating Rayleigh fractionation ($\alpha = 1.009$) (Clark and Fritz, 1997). Water samples taken at various locations in wetlands (inlet, center, and outlet).
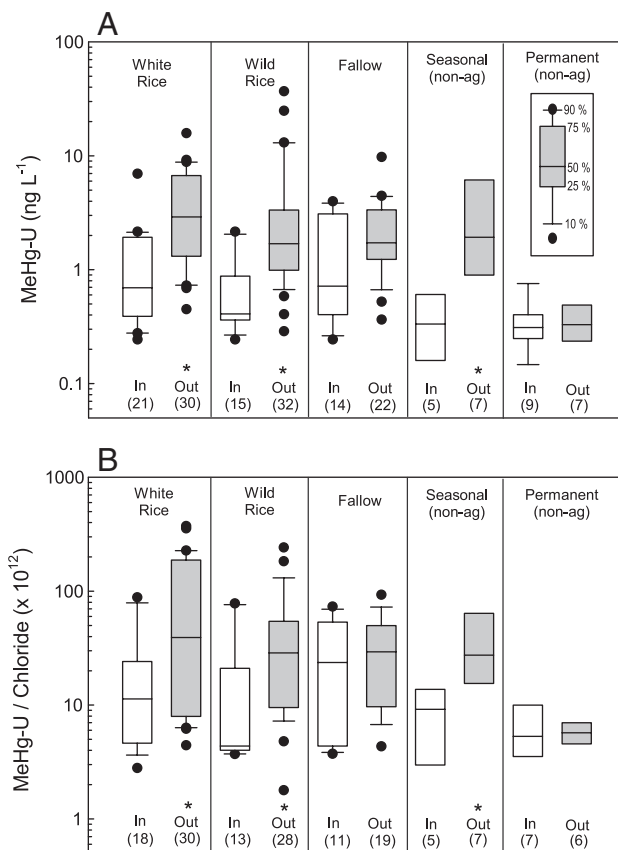

Fig. 3. Box plots comparing concentrations of inflows with outflows in surface water from various field types in agricultural and non-agricultural wetlands in the Yolo Bypass Wildlife Area, California. A) Unfiltered methylmercury (MeHg-U), and B) ratio of MeHg-U to chloride. Number of observations for each field type indicated in parentheses (at bottom). Asterisks (near label "Out") indicate a statistically significant difference (p < 0.05) between inflow and outflow data based on Mann–Whitney rank sum test.

because of a longer water residence time (Bachand et al., in this issue-a), and deeper open water without shading or vegetation compared to the agricultural fields (Fleck et al., in this issue). On fallow fields, relatively shallow water (<10 cm deep, compared with about 20 cm deep in white and wild rice fields) was maintained to optimize habitat for shore birds. During the first several weeks of inundation, flow did not reach the outlet; thus, the fallow fields did not approach steady-state conditions as readily as the other agricultural wetlands. Also, the relatively shallow water depth and lack of vegetation were more conducive for light penetration to the sediment–water interface, causing more effective photodegradation of MeHg (Fleck et al., in this issue).

An important variable controlling net MeHg export from all wetland types during the agricultural production period (summer) was [MeHg-U] in the irrigation source waters. During irrigation season, the North Supply Ditch and the Davis Drain, which supplied water to fields F20, R31, and W32, had consistently higher [MeHg-U] (median 1.14 ng L^{-1}, interquartile range 0.69 to 1.88 ng L^{-1}) than the South Supply Ditch, which supplied fields R64, W65, and F66 (median 0.37 ng L^{-1}, interquartile range 0.28 to 0.41 ng L^{-1}) (Table S5.1, Fig. S8). These differences in input water quality affected the apparent net MeHg production among agricultural fields, as computed by Bachand et al. (in this issue-b). Irrigation water already high in MeHg reduces the diffusion rate of MeHg from the soil, the primary source of MeHg to the water column (Bachand et al., in this issue-a,-b), and promotes the loss of MeHg from the water column via particle settling, advection into the soil via transpiration demand, MeHg photodegradation, and possibly microbial degradation of MeHg. Export of MeHg from agricultural wetlands during summer could thus be minimized by the utilization of irrigation water already high in MeHg, if the option is available.

3.2. Biogeochemistry affecting mercury methylation

The complexities of Hg cycling can be explained in part by relationships between Hg and S, Fe, and Mn, all of which are redox-active constituents that are affected by microbial activity.

3.2.1. Sulfur

Sulfate-reducing bacteria (SRB) are thought to play a major role in Hg(II)-methylation in many environments (Compeau and Bartha, 1984). At high H_2S concentrations, Hg(II)-methylation can be mitigated (Gilmour et al., 1998) due to the formation of non-neutral Hg-S species (Benoit et al., 2001), or the strong binding of Hg(II) mineral phases containing reduced S (Marvin-DiPasquale and Agee, 2003; Marvin-DiPasquale et al., 2009). Because SO_4^{2-} was added to the white and wild rice fields as part of fertilizer applications, possible effects on Hg cycling were investigated. The temporal trend in all agricultural wetlands during the summer months was toward lower $[SO_4^{2-}]/[Cl^-]$ values (Fig. S6A). One explanation for the observed decrease in $[SO_4^{2-}]/[Cl^-]$ during the period June through September 2007 is the reduction of SO_4^{2-} to H_2S by SRB. In some situations, stable isotopes of sulfur can provide a tracer for sulfur cycling processes, as well as for sources of sulfur (e.g. Seal et al., 2000). During periods of active sulfate reduction, the residual sulfate becomes progressively enriched in ^{34}S because ^{32}S is kinetically favored, resulting in larger values of $\delta^{34}S_{SO4}$.

The SO_4^{2-}-based fertilizer products used on the white and wild rice fields (119–268 kg SO_4 ha^{-1}, primarily as $(NH_4)_2SO4$ or $ZnSO_4$) had $\delta^{34}S_{SO4}$ values ranging from 1.2 to 8.3‰ (Table S5.10). The fertilizers were applied in mixtures such that weighted average $\delta^{34}S$ values ranged from 2.5 to 4.0‰ (Table S5.11, Fig. 4). Source water in supply canals and field inlets had $\delta^{34}S_{SO4}$ values ranging from about −2 to +2‰ (Fig. 4A). Aqueous SO_4^{2-} from some of the water samples from field centers and outlets had $\delta^{34}S$ values greater than 4.0‰ (Fig. 4A), indicating that sulfate reduction was active; the activity of SRB is the only plausible explanation for the elevated values of $\delta^{34}S_{SO4}$ as sulfur isotope ratios are not influenced by evapoconcentration. Active sulfate reduction during
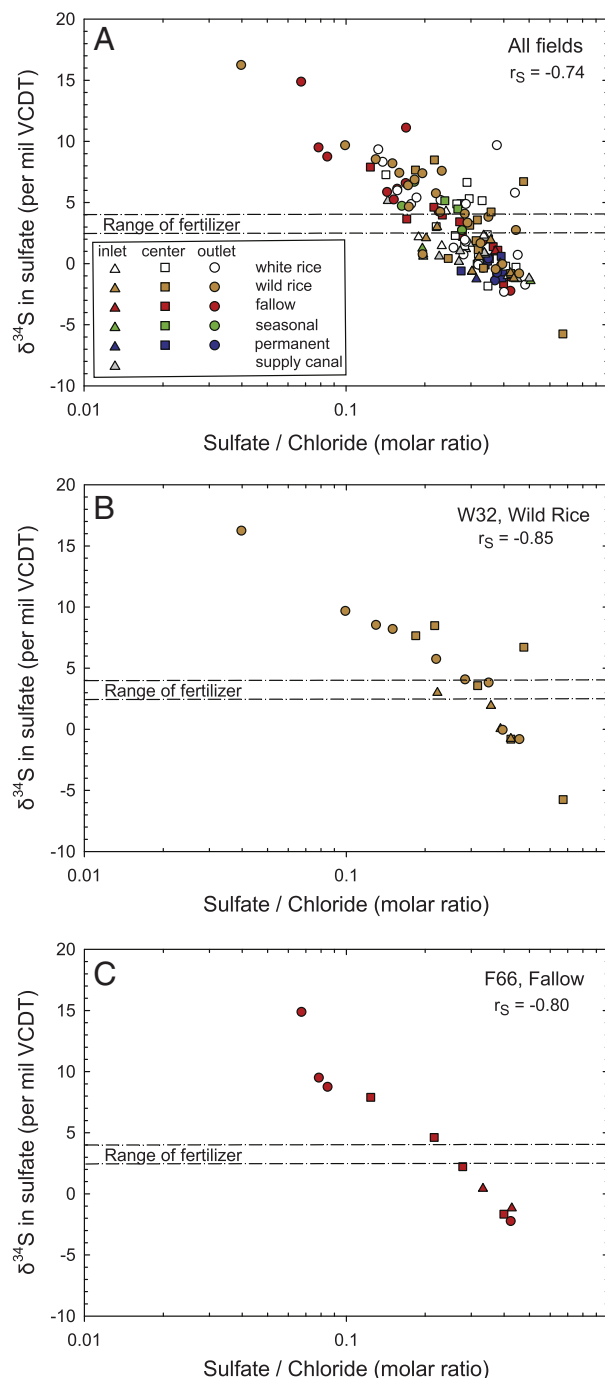

Fig. 4. Plots showing relationships between ratio of sulfate to chloride concentration in filtered water samples and $\delta^{34}S$ of aqueous sulfate for surface-water samples from agricultural and non-agricultural wetlands in the Yolo Bypass Wildlife Area, California. A) All sites, B) field W32 (wild rice), C) field F66 (fallow). Values of r_S are Spearman rank order coefficients. All correlations are statistically significant (p < 0.001). Dashed lines show range of $\delta^{34}S$ values for sulfate-bearing fertilizer applied to agricultural fields during 2007 growing season.

flooded conditions on the fields in the YBWA was also indicated by radiotracer (^{35}S) incubations of sediment (Marvin-DiPasquale et al., in this issue). It is not known whether the SRB activity occurred exclusively in the sediment, or whether there may have been transient activity in biofilms or microzones that were anoxic (e.g. Fry and Chumchal, 2012). The latter may have been important given that diffusive flux from sediment may have been too slow to account for all of the SRB activity observed.

A significant inverse correlation ($r_S = -0.74$, $p < 0.001$) was found between $[SO_4^{2-}]/[Cl^-]$ and $\delta^{34}S$ for all water samples (Fig. 4A). This relationship held ($p < 0.05$) on all eight fields (Table S8A), with r_S values ranging from -0.33 to -0.85 (see two examples in Fig. 4B and C). These data provide additional evidence that SRB were actively removing sulfate from the water column. Decreases in $[SO_4^{2-}]/[Cl^-]$ and coupled increases in $\delta^{34}S$ can each be considered indicators of sulfate reduction in the YBWA wetlands. Furthermore, it is unlikely that interactions between sulfate and plants are responsible for the variations in aqueous $\delta^{34}S$, because isotope fractionation during plant uptake of sulfate is minimal (Trust and Fry, 1992). To achieve a shift in $\delta^{34}S$ values of $+10‰$, approximately the range observed on most fields (Fig. 4), about 20% of the sulfate would need to have been reduced, assuming a closed system (Seal et al., 2000). In an open system, an even higher proportion of sulfate would need to be reduced to show the same amount of ^{34}S enrichment. The fields are not closed systems, in that mass transfer between geochemical reservoirs (i.e. sediment, pore water, surface water, biofilm, etc.) is likely occurring to some extent, so we conclude that more than 20% of the sulfate was reduced.

Because SRB have been frequently mentioned in the literature as the main microbial consortium responsible for Hg methylation in wetlands (e.g. Gilmour et al., 1992), including rice paddies (e.g. Rothenberg and Feng, 2012), the quantitative relations between ($[SO_4^{2-}]/[Cl^-]$, $\delta^{34}S$, [MeHg-U] and [MeHg-F]) are of interest. Values of r_S for the correlations of $[SO_4^{2-}]/[Cl^-]$ with [MeHg-U] and with [MeHg-F] were -0.27 and -0.26, respectively; r_S values for $\delta^{34}S$ with [MeHg-U] and [MeHg-F] were 0.39 and 0.26, respectively (Table 2). Absolute values of r_S for the correlation of $[SO_4^{2-}]/[Cl^-]$ and $\delta^{34}S$ with MeHg/THg in both unfiltered and filtered water were in a similar range (0.30 to 0.40; Table 2).

Data for individual wetlands indicate a significant correlation between $\delta^{34}S$ and [MeHg-U] for four of eight wetlands, however, significant correlations between $[SO_4^{2-}]/[Cl^-]$ and various MeHg parameters ([MeHg-U], [MeHg-F], and MeHg/THg in both unfiltered and filtered water) were observed in only one or two of eight wetlands (Table S8).

In summary, the water-quality data in this study indicate significant, but relatively weak correlations between concentrations of aqueous MeHg species and some parameters that are indicative of sulfate reduction, namely $[SO_4^{2-}/Cl^-]$ and $\delta^{34}S_{SO4}$ (Table 2). These results are consistent with SRB playing a direct role in Hg(II)-methylation. In the following section we explore other geochemical parameters that correlate with MeHg and may provide additional insight into Hg cycling in YWBA wetlands.

3.2.2. Iron and manganese

Prior to 2006, there was a general consensus in the literature that Hg(II)-methylation was microbially mediated in most environmental settings, and that SRB are the main participants (e.g. Compeau and Bartha, 1984; Gilmour et al., 1992, 2011). Studies using molybdate inhibition have shown that some iron-reducing bacteria (FeRB), such as strains of *Geobacter* and *Desulfuromonas*, can also be responsible for Hg(II)-methylation (e.g. Fleming et al., 2006; Kerin et al., 2006). Other researchers have suggested that Fe(II) may scavenge H_2S produced by SRB, making Hg(II) available for methylation even in sulfidic conditions (Gagnon et al., 1996; Hammerschmidt and Fitzgerald, 2004). *Geobacter sulfurreducens* has been shown to have a high Hg(II)-methylation rate in the presence of cysteine (Schaefer and Morel, 2009). Recent advances regarding the genetic basis for microbial Hg(II)-methylation (Parks et al., 2013) indicate that a variety of microbes (including reducers of sulfate, iron, and uranium as well as methanogenic bacteria) have the genetic machinery capable of methylating Hg(II). The sediment component of this study found that SRB are dominant in the permanent wetland but that conditions generally favor FeRB in the seasonal and agricultural wetlands (Marvin-DiPasquale et al., in this issue).

Because FeRB (and possibly manganese-reducing bacteria, MnRB) also have been identified as possible contributors to Hg(II)-methylation,

we explored the relations between [Fe], [Mn], and [MeHg] in the water-quality data. In the circum-neutral pH range of YBWA surface waters (Table S5.1), Fe is likely to occur primarily as Fe(II) and Mn as Mn(II) because the more oxidized forms (Fe(III), Mn(III), and Mn(IV)) are relatively insoluble in this pH range (Langmuir, 1997). In wetlands, Fe(II) is produced by reduction of Fe(III) by dissimilitory Fe reduction; similarly, Mn(II) is produced by reduction of Mn(III) and Mn(IV) by dissimilitory Mn reduction (Lovley, 1991; Lovley et al., 2004). Because Fe(II) and Mn(II) represent the end products of FeRB and MnRB, surface water concentrations of these constituents provide an indication of the extent to which Fe reduction and Mn reduction have occurred. Although the location of Fe and Mn reduction is not known, it could be in the water column, in shallow sediment, or in biofilm.

The fact that comparable correlations were observed between MeHg and [Fe] (Table 2) compared with correlations between MeHg and indicators of sulfate reduction suggest that FeRB may also play a direct role in Hg(II) methylation within the field area, although to a lesser extent within the permanent wetland. The wet/dry cycle in seasonal and agricultural wetlands re-oxidizes Fe(II) to Fe(III), providing an electron acceptor for FeRB. In permanent wetlands that are hydrologically more stable, there are no wet/dry cycles and concentrations of Fe(III) in sediment (0–2 cm depth) are much lower than in the agricultural fields (Marvin-DiPasquale et al., in this issue). Because there was abundant sulfate in the inlet waters feeding all the study wetlands, SRB were not sulfate-limited, and sulfate reduction could proceed in all wetlands, including the permanent wetland that did not experience wet/dry cycles. Bed sediment samples collected at field centers in this study (Marvin-DiPasquale et al., in this issue) demonstrated a negative correlation between total reduced sulfur (TRS) and reactive mercury (Hg(II)$_R$), suggesting that solid-phase reduced sulfur may partially control Hg(II) availability for methylation by SRB or FeRB.

Considering data from all wetlands, a relatively weak, though statistically significant positive correlation ($r_S = 0.29$, $p < 0.05$) was observed between [Fe] and [MeHg-U], whereas the correlation between [Mn] and [MeHg-U] was much stronger ($r_S = 0.66$, $p < 0.001$) (Table 2, Fig. S10A). At the level of wetland type, the positive correlation between [Mn] and [MeHg-U] was strongest for white rice (Fig. S10B, $r_S = 0.78$; $p < 0.001$), whereas the correlation for wild rice fields was somewhat weaker (Fig. S10C, $r_S = 0.62$; $p < 0.001$). Correlations between [Mn] and [MeHg-F] were also relatively strong across all wetland types ($r_S = 0.67$; $p < 0.001$). Testing a possible predictive relationship between [Mn] and [MeHg-F] via linear least-squares regression gives yields a coefficient of determination (r^2) of 0.51 (Fig. 5A). Six of eight individual wetlands showed significant correlations ($p < 0.1$) between [Mn] and [MeHg-F], with r_S values ranging from 0.48 to 0.91 (Table S8); possible predictive relationships for three agricultural fields have r^2 values ranging from 0.76 to 0.81 and p values < 0.001 (Fig. 5B–D).

The correlations between [Mn] and MeHg species (Figs. 5, S10) are stronger than those involving [Fe], $[SO_4^{2-}/Cl^-]$ and $\delta^{34}S_{SO4}$ (Table 2). The observed correlations between [Mn] and MeHg species suggest the possibility that MnRB may play a role in Hg(II)-methylation. A few other studies have shown correlations between Mn and MeHg. Balogh et al. (2004) showed increased dissolved Mn and Fe in Minnesota streams during periods of increased MeHg concentration in surface-waters, which they attributed to reducing conditions. Gill (2008) showed significant correlations between MeHg and dissolved Fe and Mn in pore water from two tidal marshes in the San Francisco Bay-Delta. Manganese may also have indirect effects on cycling of other redox-sensitive elements including Fe, S, and Hg. For example the addition of Mn(IV) (or nitrate) to rice paddy soils inhibited Fe(III) reduction and concomitantly remedied physiological disorders in rice plants (Yuan and Ponnamperuma, 1966; Lovley, 1991).

Although the correlations observed between [Mn] and MeHg species in our study are intriguing, they do not necessarily imply causation with regard to the MnRB being directly involved in Hg(II)-methylation. It is

possible that the elevated [Mn] in wetland waters may simply be an effect of reducing conditions that are suitable for anaerobic microbes, including SRB and FeRB, which are known to methylate Hg(II).

4. Summary and conclusions

Concentrations of THg and MeHg in surface water were highly variable, both spatially and seasonally, in agricultural and non-agricultural wetland types studied. Both THg and MeHg ranged over approximately two orders of magnitude in filtered and unfiltered water. The highest MeHg-U concentrations (up to 37 ng L^{-1}), among the highest ever recorded in wetlands, were observed at outlets during the wild rice harvest; harvesting this crop during wet conditions caused export of MeHg from these fields. Another period of elevated MeHg-U concentration (4–9 ng L^{-1}) was during the regional flood on white rice fields. The decomposition of rice straw during this period contributed labile organics (e.g. acetate; Windham-Myers et al., in this issue-b,-c) that stimulated microbial activity, including Hg(II)-methylation.

Concentrations of MeHg on suspended particulate matter in the water column were about ten-fold higher than MeHg in the top (0–2 cm) of bed sediment (Marvin-DiPasquale et al., in this issue). There was a significant correlation between the organic content of SPM (measured as LOI) and the MeHg concentration of suspended particulates, consistent with uptake of MeHg onto phytoplankton and (or) suspended organic detritus representing periphyton or biofilm from sediment or plant surfaces.

There were several systematic differences in water quality between the permanent wetland and the agricultural wetlands. During the rice-growing season, agricultural wetlands exhibited dramatic increases (about 20-fold) in MeHg/THg in both filtered and unfiltered water (at field centers and outlets), while there was little to no change in these ratios in the permanent wetland. Concentration of MeHg-U increased significantly from inlet to outlet in the white rice, wild rice, and seasonal (non-agricultural) wetlands, while no significant increase in MeHg-U was observed from inlet to outlet in the permanent wetland or the fallow agricultural wetlands.

Sulfate reduction occurred in all wetlands based on decreases in [SO$_4^{2-}$]/[Cl$^-$] and increases in δ^{34}S$_{SO4}$. The input waters to the YWBA wetlands had sufficiently high sulfate concentration that SRB were not sulfate-limited during the study. Thus, addition of sulfate-bearing fertilizers to the white and wild rice fields had no apparent effect on SRB activity or on MeHg concentrations, consistent with results for sediment and pore water in this study (Marvin-DiPasquale et al., in this issue).

Concentrations of Fe and Mn in filtered water, presumably occurring predominantly as dissolved Fe(II) and Mn(II), increased with duration of wetland inundation indicating activity of FeRB and MnRB. Values of MeHg/THg in both filtered and unfiltered water increased along with Fe and Mn in the agricultural wetlands; however, these patterns were not observed in the permanent wetland. Correlations between Mn and various MeHg species (including MeHg/THg ratios) were stronger than correlations with Fe or various indicators of sulfate reduction. Future work relating biogeochemical processes in pore water to the overlying water column would be helpful in resolving these processes. Additional studies are warranted to determine whether MnRB can methylate Hg directly. In the absence of such evidence, Mn concentration should be considered as a sensitive indicator of reducing conditions in which FeRB and (or) SRB are likely responsible for Hg(II)-methylation.
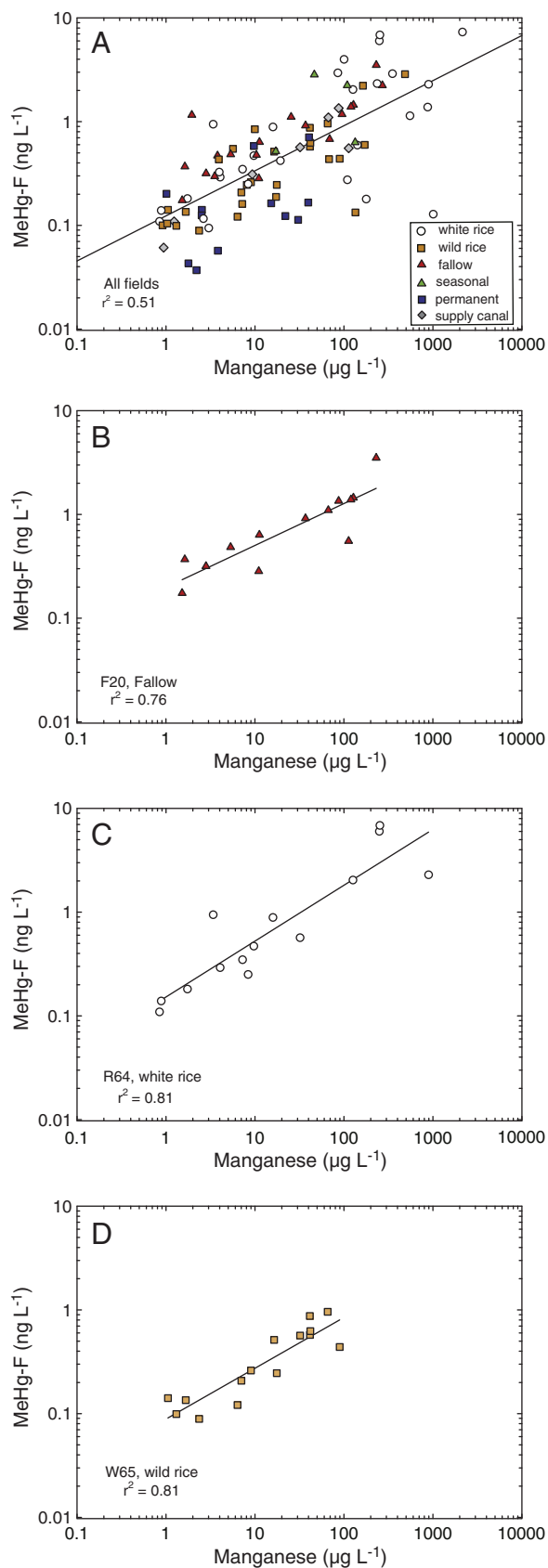
Fig. 5. Plots showing relationships between concentrations of manganese in filtered water and methylmercury in unfiltered water in surface-water samples from agricultural and non-agricultural wetlands in the Yolo Bypass Wildlife Area, California. A) All samples, B) fallow field F20, C) white rice field R64, D) wild rice field W65. Values of r^2 from linear least-squares regressions.

Appendix A. Supplementary data

Supplementary data to this article can be found online at http://dx.doi.org/10.1016/j.scitotenv.2013.10.096.

References

Ackerman JT, Eagles-Smith CA. Agricultural wetlands as potential hotspots for bioaccumulation: experimental evidence using caged fish. Environ Sci Technol 2010;44: 1451–7.

Ackerman JT, Takekawa JY, Eagles-Smith CA, Iverson SA. Mercury contamination and effects on survival of American avocet and black-necked stilt chicks in San Francisco Bay. Ecotoxicology 2008;17:103–16.

Ackerman JT, Miles AK, Eagles-Smith CA. Invertebrate mercury bioaccumulation in permanent, seasonal, and flooded rice wetlands within California's Central Valley. Sci Total Environ 2010;408:666–71.

Alpers CN, Hunerlach MP, May JT, Hothem RL. Mercury contamination from historical gold mining in California. U S Geol Surv Fact Sheet 2005;3014:1–6. [http://water.usgs.gov/pubs/fs/2005/3014/].

Alpers CN, Stewart AR, Saiki MK, Marvin-DiPasquale MC, Topping BR, Rider KM, et al. Environmental factors affecting mercury in Camp Far West Reservoir, 2001–03. U S Geol Surv Sci Investig Rpt 2008;2006-5008. [358 pp.].

Bachand PAM, Bachand S, Fleck JA, Anderson F, Windham-Myers L. Hydrologic modeling for quantifying aqueous fluxes in shallow seasonal wetlands: why internal flowpaths are critical to understanding temporal mercury cycling; 2013a [in this issue-a].

Bachand PAM, Fleck JA, Bachand S, Anderson F, Stephenson M, Alpers CN. Methylmercury production and export from agricultural wetlands (rotational rice) in California. USA: revelations from hydrologic analyses; 2013b [in this issue-b].

Balogh SJ, Nollet YH, Swain EB. Redox chemistry in Minnesota streams during episodes of increased methylmercury discharge. Environ Sci Tech 2004;38:4921–7.

Balogh SJ, Swain EB, Nollet YH. Characteristics of mercury speciation in Minnesota rivers and stream. Environ Pollut 2008;154:3–11.

Benoit JM, Gilmour CC, Mason RP. The influence of sulfide on solid-phase mercury bioavailability for methylation by pure cultures of *Desulfobulbus propionicus* (1pr3). Environ Sci Technol 2001;35:127–32.

Bergamaschi BA, Fleck JA, Downing BD, Boss E, Pellerin B, Ganju NK, et al. Methyl mercury dynamics in a tidal wetland quantified using in situ optical measurements. Limnol Oceanogr 2011;56:1355–71.

Bradley PM, Burns DA, Riva-Murray K, Brigham ME, Button DT, Chasar LC, et al. Spatial and seasonal variability of dissolved methylmercury in two stream basins in the eastern United States. Environ Sci Technol 2011;45:2048–55.

Brigham ME, Wentz DA, Aiken GR, Krabbenhoft DP. Mercury cycling in stream ecosystems. 1. Water column chemistry and transport. Environ Sci Technol 2009;43:2720–5.

California Rice Commission. California rice's growing region. http://www.calrice.org/Industry+Info/About+California+Rice/California+Rice+Growing+Region.htm, 2012. [accessed July 21, 2012].

California Wild Rice Advisory Board. Facts about California wild rice. http://cawildrice.com/wild-rice-facts.php, 2012. [accessed Sept. 30, 2013].

Carmody RW, Plummer LN, Busenberg E, Coplen TP. Methods for collection of dissolved sulfate and sulfide and analysis of their sulfur isotopic composition. U.S. Geological Survey Open-File Report 97-234; 1998 [91 pp.].

Central Valley Joint Venture. Central Valley Joint Venture implementation plan — conserving bird habitat. Sacramento, CA: U.S. Fish and Wildlife Service; 2006 [http://www.centralvalleyjointventure.org/assets/pdf/CVJV_fnl.pdf (accessed July 21, 2012)].

Clark I, Fritz P. Environmental isotopes in hydrogeology. New York: Lewis Publishers; 1997 [328 pp.].

Coleman ML, Shepherd TJ, Durham JJ, Rouse JE, Moore GR. Reduction of water with zinc for hydrogen isotope analysis. Anal Chem 1982;54(6):993–5. http://dx.doi.org/10.1021/ac00243a035.

Compeau G, Bartha R. Methylation and demethylation of mercury under controlled redox, pH, and salinity conditions. Appl Environ Microbiol 1984;50:498–502.

Craig H. Isotopic variations in meteoric waters. Science 1961;133:1702–3.

Davis JA, Yee D, Collins JN, Schwarzbach SE, Louma SN, Davis JA, et al. Potential for increased mercury accumulation in the estuary food web. In: Brown LR, editor. Issues in San Francisco estuary tidal wetlands restoration, 1(1). San Francisco estuary and watershed science; 2003. [art 4 http://repositories.cdlib.org/jmie/sfews/vol1/iss1/art4 (accessed Sept. 30, 2010)].

Domagalski JL, Alpers CN, Slotton DG, Suchanek TH, Ayers SM. Mercury and methylmercury concentrations and loads in the Cache Creek Watershed, California. Sci Total Environ 2004;327:215–37.

Drever JI. The geochemistry of natural waters: surface and groundwater environments. 3rd ed. Upper Saddle River, New Jersey: Prentice Hall, Inc.; 1997 [436 pp.].

Elphick CS. Functional equivalency between rice fields and seminatural wetland habitats. Conserv Biol 2000;14:1–13.

Epstein S, Mayeda T. Variation of ^{18}O content of waters from natural sources. Geochim Cosmochim Acta 1953;4:213–24.

Fitzgerald WF, Lamborg CH. Geochemistry of mercury in the environment. Treatise of Geochemistry, 9.04. Elsevier Ltd.; 2007. p. 1–47.

Fleck JA, Gill G, Downing BD, Bergamaschi BA, Alpers CN. Concurrent photodegradation of dissolved organic matter and methylmercury and its effect on their relationship in natural waters; 2013 [in this issue].

Fleming EJ, Mack EE, Green PG, Nelson DC. Mercury methylation from unexpected sources: molybdate-inhibited freshwater sediments and an iron-reducing bacterium. Appl Environ Microbiol 2006;72:457–64.

Fry B, Chumchal MM. Mercury bioaccumulation in estuarine food webs. Ecol Appl 2012;22:606–23.

Gagnon CE, Pelletier A, Mucci A, Fitzgerald WF. Diagenetic behavior of methylmercury in organic rich coastal sediments. Limnol Oceanogr 1996;41:428–34.

Ganguli PM, Mason RP, Abu-Saba KE, Anderson RS, Flegal AR. Mercury speciation in drainage from the New Idria mercury mine, California. Environ Sci Technol 2000;34:4773–9.

Gill G. Monomethylmercury photo-degradation studies. Transport, cycling, and fate of mercury and monomethylmercury in the San Francisco Delta and tributaries: an integrated mass balance assessment approach: final report to the California Department of Fish and Game and the California Bay Delta Authority, Task 5.1. 2008. [21 pp. http://mercury.mlml.calstate.edu/wp-content/uploads/2008/10/09_task5_1_final.pdf (accessed Sept. 30, 2010)].

Gilmour CC, Henry EA, Mitchell R. Sulfate stimulation of mercury methylation in freshwater sediments. Environ Sci Technol 1992;26:2281–7.

Gilmour CC, Riedel GS, Ederington MC, Bell JT, Benoit JM, Gill GA, et al. Methylmercury concentrations and production rates across a trophic gradient in the northern Everglades. Biogeochemistry 1998;40:327–45.

Gilmour CC, Elias DA, Kucken AM, Brown SD, Palumbo AV, Schadt CW, et al. Sulfate-reducing bacterium *Desulfovibrio desulfuricans* ND132 as a model for understanding bacterial mercury methylation. Appl Environ Microbiol 2011;77:3938–51. http://dx.doi.org/10.1128/AEM.02993-10.

Gray JE, Crock JG, Lasorsa BK. Mercury methylation at mercury mines in the Humboldt River basin, Nevada, USA. Geochem Explor Environ Anal 2002;2:143–9.

Gray JE, Hines ME, Higueras PL, Adatto I, Lasorsa BK. Mercury speciation and microbial transformations in mine wastes, river sediments, and surface waters at the Almadén mining district, Spain. Environ Sci Technol 2004;38:4285–92.

Guentzel J. Wetland influences on mercury transport and bioaccumulation in South Carolina. Sci Total Environ 2009;407:1344–53.

Hammerschmidt CR, Fitzgerald WF. Geochemical controls on the production and distribution of methylmercury in near-shore marine sediments. Environ Sci Technol 2004;38:1487–95.

Heim W, Coale K, Stephenson M, Choe K-Y, Gill G, Foe C. Spatial and habitat-based variations in total and methyl mercury concentrations in surficial sediments in the San Francisco Bay-Delta. Environ Sci Technol 2007;41:3501–7.

Horvat M, Nolde N, Fajon V, Jereb V, Logar M, Lojen S, et al. Total mercury methylmercury and selenium in mercury polluted areas in the province Guizhou, China. Sci Total Environ 2003;304:231–56.

Jeremiason JD, Engstrom DR, Swain EB, Nater EA, Johnson BM, Almendinger JE, et al. Sulfate addition increases methylmercury production in an experimental wetland. Environ Sci Technol 2006;40:3800–6.

Kerin E, Gilmour CC, Roden E, Suzuki MT, Coates JD, Mason RP. Mercury methylation among the dissimilatory iron-reducing bacteria. Appl Environ Microbiol 2006;72: 7919–21.

Kester CL, Rye RO, Johnson CA, Schwartz CH, Holmes CH. On-line sulfur isotope analysis of organic material by direct combustion: preliminary results and potential applications. Isotopes Environ Health Stud 2001;37:53–65.

Krabbenhoft DP, Wiener JG, Brumbaugh WG, Olson ML, DeWild JF, Sabinal TJ. A national pilot study of mercury contamination of aquatic ecosystems along multiple gradients. In: Morganwalp DW, Buxton HT, editors. U.S. Geological Survey toxic substances hydrology program — proceedings of the technical meeting, Charleston, SC, March 8–12, 1999 — volume 2 of 3 — contamination of hydrologic systems and related ecosystems, 99-4018. USGS Water-Res Invest Rpt; 1999. p. 147–60. [Available at: http://toxics.usgs.gov/pubs/wri99-4018/Volume2/sectionB/2301_Krabbenhoft/pdf/2301_Krabbenhoft.pdf (accessed: August, 2007)].

Langmuir D. Aqueous environmental chemistry. Upper Saddle River, New Jersey: Prentice Hall; 1997 [600 pp.].

Lin C-C, Jay JA. Mercury methylation by planktonic and biofilm cultures of *Desulfovibrio desulfuricans*. Environ Sci Tech 2007;41:6691–7.

Lovley DR. Dissimilatory Fe(III) and Mn(IV) reduction. Microbiol Rev 1991;55:259–87.

Lovley DR, Holmes DE, Nevin DP. Dissimilatory Fe(III) and Mn(IV) reduction. Adv Microb Physiol 2004;49:219–86.

Marvin-DiPasquale M, Alpers CN, Fleck JA. Mercury, methylmercury, and other constituents in sediment and water from seasonal and permanent wetlands in the Cache Creek Settling Basin and Yolo Bypass, Yolo County, California, 2005–06. U.S. Geol Surv, Open File Report 2009-1182; 2009 [69 pp. http://pubs.usgs.gov/of/2009/1182/ (accessed Sept. 30, 2010)].

Marvin-DiPasquale M, Agee JL. Microbial mercury cycling in sediments of the San Francisco Bay-Delta. Estuaries 2003;26:1517–28.

Marvin-DiPasquale M, Windham-Myers L, Agee JL, Kakouros E, Kieu LH, Fleck JA, Alpers CN, Stricker CA. Methylmercury production in sediment from agricultural and non-agricultural wetlands in the Yolo Bypass, California; 2013 [in this issue].

Orem W, Gilmour C, Axelrad D, Krabbenhoft D, Scheidt D, Kalla P, et al. Sulfur in the South Florida Ecosystem: distribution, sources, biogeochemistry, impacts, and management for restoration. Crit Rev Environ Sci Technol 2011;41(S1):249–88.

Parks JM, Johs A, Podar M, Bridou R, Hurt Jr RA, Smith SD, et al. The genetic basis for bacterial mercury methylation. Science 2013;339(6125):1332–5. http://dx.doi.org/10.1126/science.1230667.

Pickhard PC, Fisher NS. Accumulation of inorganic and methylmercury by freshwaterphytoplankton in two contrasting water bodies. Environ Sci Tech 2007;41:125–31.

Rothenberg SE, Feng X. Mercury cycling in a flooded rice paddy. J Geophys Res 2012;117. http://dx.doi.org/10.1029/2011JG001800. G03003.

Rudd JWM. Sources of methyl mercury to freshwater ecosystems: a review. Water Air Soil Pollut 1995;80:697–713.

Rumbold DG, Fink LE. Extreme spatial variability and unprecedented methylmercury concentrations within a constructed wetland. Environ Monit Assess 2006;112:115–35.

Rytuba JJ. Mercury from mineral deposits and potential environmental impact. Environ Geol 2003;43:326–38.

Schaefer JK, Morel FMM. High methylation rates of mercury bound to cysteine by Geobacter sulfurreducens. Nat Geosci 2009;2:123–6.

Seal II RR, Alpers CN, Rye RO. Stable isotope systematics of sulfate minerals. In: Alpers CN, Jambor JL, Nordstrom DK, editors. Rev Mineral Geochem, 40. Washington, D.C.: Mineralogical Society of America and Geochemical Society; 2000. p. 541–602.

Snodgrass JW, Jagoe CH, Bryan AL, Brant HA, Burger J. Effects of trophic status and wetland morphology, hydroperiod, and water chemistry on mercury concentrations in fish. Can J Fish Aquat Sci 2011;57:171–80.

Sommer TR, Harrell WC, Swift TJ. Extreme hydrologic banding in a large-river floodplain, California. U S A Hydrobiol 2008;598:409–15.

Springborn M, Singer MB, Dunne T. Sediment-adsorbed total mercury flux through Yolo Bypass, the primary floodway and wetland in the Sacramento Valley, California. Sci Total Environ 2011;412:203–13.

St. Louis VL, Rudd JWM, Kelly CA, Beaty KG, Bloom NS, Flett RJ. Importance of wetlands as sources of methylmercury to boreal forest ecosystems. Can J Fish Aquat Sci 1994;51:1065–76.

St. Louis VL, Rudd JWM, Kelly CA, Beaty KG, Robert JF, Roulet NT. Production and loss of methylmercury and loss of total mercury from boreal forest catchments containing different types of wetlands. Environ Sci Technol 1996;30:2719–29.

Trust BA, Fry B. Stable sulfur isotopes in plants — a review. Plant Cell Environ 1992;15:1105–10.

Turner A, Millward GE. Suspended particles: their role in estuarine biogeochemical cycles. Estuar Coast Shelf Sci 2002;55:857–83.

U.S. Environmental Protection Agency (EPA). Water quality standards — establishment of numeric criteria for priority toxic pollutants for the State of California, 40 CFR part 131. http://www.epa.gov/fedrgstr/EPA-WATER/2000/May/Day-18/w11106.pdf, [accessed Sept. 30, 2010].

Windham-Myers L, Fleck JA, Ackerman JT, Marvin-DiPasquale M, Stricker CA, Heim WA, et al. Mercury cycling in agricultural and managed wetlands: a synthesis of methylmercury production, hydrologic export, and bioaccumulation from an integrated field study; 2013a [in this issue-a].

Windham-Myers L, Marvin-DiPasquale M, Stricker C, Agee JL, Kieu LH, Kakouros E. Mercury cycling in agricultural and managed wetlands, Yolo Bypass, California: vegetation influences on methylmercury production; 2013b [in this issue-b].

Windham-Myers L, Marvin-DiPasquale M, Kakouros E, Agee JL, Kieu LH, Stricker C, et al. Mercury cycling in agricultural and managed wetlands, Yolo Bypass, California: vegetation influences on methylmercury storage, export, and bioaccumulation; 2013c [in this issue-c].

Wood ML, Morris P, Cooke J, Louie SJ. Amendments to the water quality control plan for the Sacramento River and San Joaquin River basins for the control of methylmercury and total mercury in the Sacramento–San Joaquin Delta estuary: staff report, Regional Water Quality Control Board — Central Valley Region; 2010 [April, 332 pp. http://www.swrcb.ca.gov/rwqcb5/water_issues/tmdl/central_valley_projects/delta_hg/april_2010_hg_tmdl_hearing/index.shtml (accessed Sept. 30, 2010)].

Yuan WL, Ponnamperuma FN. Chemical retardation of the reduction of flooded soils and the growth of rice. Plant Soil 1966;25:347–60.

Zhang T, Kim B, Levard C, Reinsch BC, Lowry GV, Deshusses MA, et al. Methylation of mercury by bacteria exposed to dissolved, nanoparticulate, and microparticulate mercuric sulfides. Environ Sci Tech 2012;46:6950–8.